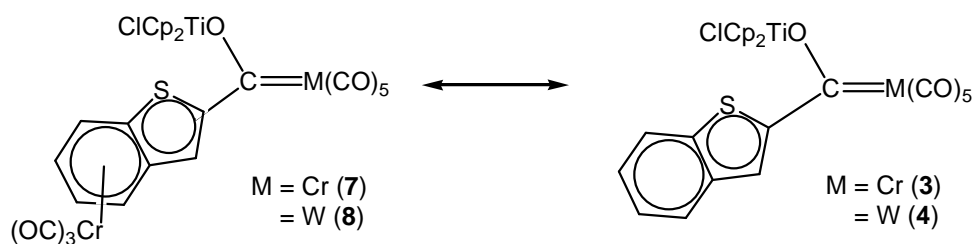


# 6 Conclusion

## 1. Stability of complexes

The stabilities of the complexes **1–8** were not formally investigated, but the rates of decomposition of the different complexes in solution and on exposure to air were used as criteria. It was found that the stability of the complexes decreased on increasing the number of metal fragments surrounding the carbene carbon atom. For instance, the carbene complexes containing three metal fragments decomposed within hours in an inert atmosphere in solution, while the analogous carbene complex containing only one metal fragment was stable for several days under the same conditions. Carbene complexes are sensitive towards oxygen and the substitution of a metal fragment by oxygen is a common occurrence in reactive carbene complexes.<sup>1-3</sup> Also, in reactive carbene complexes under inert conditions with the exclusion of oxygen or oxygen containing solvents, carbene-carbene carbon-carbon coupling reactions have been observed.<sup>4,5</sup> Neither of these two decomposition pathways were observed from studying NMR spectra in CDCl<sub>3</sub> of **5–8** that have changed their composition. The most important routes for complexes losing their identity was the substitution of the carbene ligand to afford M(CO)<sub>6</sub> complexes and the  $\pi$ -coordination mode for Cr(CO)<sub>3</sub> fragments (Scheme 6.1). The stability of the different complexes was found to follow the trend depicted in Figure 6.1 (The top complex, being the more stable one).



**Scheme 6.1**

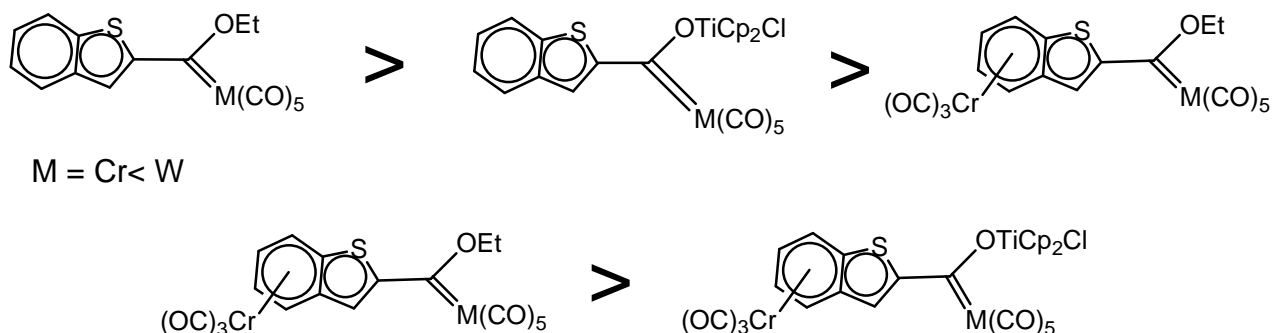


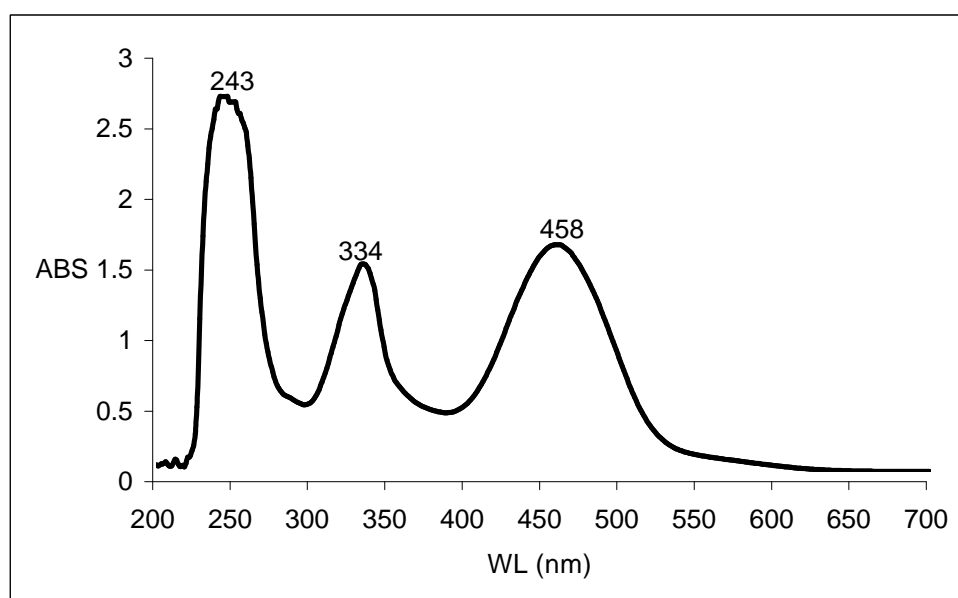
**Figure 6.1** Decreasing order for the stability of complexes **1-8**.

## 2. Electronic spectra

The UV-spectra of the complexes containing a  $W(CO)_5$ -fragment were recorded in dichloromethane. The electronic data of the series **2**, **4**, **6** and **8** are produced in Table 6.1. The electronic spectrum of complex **2** is presented by Figure 6.2. All the complexes exhibit very strong ligand-based absorption bands between 223 and 245 nm. Intense characteristic absorption bands with  $\lambda_{max}$  in the range 325 to 380 nm are assigned to the benzo[*b*]thiophene-based p-p\* transitions. In benzo[*b*]thiophene this transition is observed at 265 nm when measured in dichloromethane. Coordination to metal fragments shifts this band to higher wavelengths, indicating interaction of the metal carbene p-system with that of the thiophene substituent. This means that the energies of the p-p\* transitions in the benzo[*b*]thiophene substituent are reduced. Displacement of the p-p\* transitions to lower energies upon metallation has been observed for p-metal complexes of oligothiophenes end-capped with ruthenium units.<sup>6-8</sup> The absorption band at lowest energy is assigned to the d-p metal-to-ligand charge transfer transition. Since the colours of the different complexes are characteristic to the number of metal moieties coordinated to the carbene carbon, it is not surprising that the values of this transition are very similar for the different types of complexes. Complexes containing one metal fragment all have a red colour, those containing two metal fragments are of a darker colour varying between red-brown and purple, while the complexes containing three metal fragments are a very dark purple.

**Table 6.1** UV data of complexes **2**, **4**, **6** and **8**

Complex	Colour	Ligand p-p* transition (?, nm)	Metal-ligand transition (?, nm)
<b>2</b>	Red-brown	334	458
<b>4</b>	Red-orange	334, 381	483
<b>6</b>	Dark brown	325	449, 569
<b>8</b>	Purple	325	494, 567

**Figure 6.2** UV-spectrum of complex **2**

### 3. NMR Spectroscopy

The bridging ligands were such in **3-8** that metal-metal communication exists in all the complexes. Surrounding the  $M(CO)_5$  carbene carbon are two substituents that were chosen to create competitive demands on electrons vital to stabilize the carbene carbon atom. In all the complexes prepared in this study a flow of electron density can be recognised. For the complexes containing one metal fragment (**1** and **2**), the electron flow is from the oxygen and from the BT-substituent towards the carbene carbon, once a titanoxo-fragment is added (**3** and **4**), a competition for electron density between the positive titanium(IV) and

the carbene carbon is introduced and when a p-fragment of  $\text{Cr}(\text{CO})_3$  is added on the benzene ring, this fragment will withdraw electron density (**5** and **6**) from the BT-substituent and cause competition. Surrounding the carbene carbon atom by three metal fragments (**7** and **8**), causing push-pull effects, this will affect the whole complex (Figure 6.3), causing the most dramatic scenario. Figure 6.2 shows the flow of electron density to the carbene carbon atom as well as competitive processes by the titanocene chloride and  $\text{Cr}(\text{CO})_3$  fragments. It is clear that the metal-fragments of **7** and **8** can "communicate" electronically with each other.

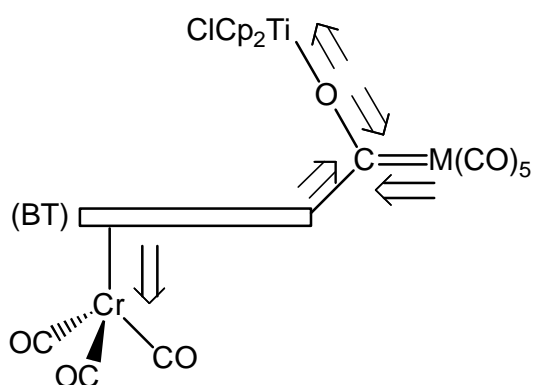


**Figure 6.3** Effect of metal fragments on electron flow in the carbene complexes **7** and **8**

**Table 6.1**  $^1\text{H}$  NMR Spectra of complexes **1-8** for the BT-substituent

Proton	Chemical shifts (d, ppm)						
	[Cr(CO) <sub>5</sub> ]-complexes			[W(CO) <sub>5</sub> ]-complexes			
	<b>1</b>	<b>3</b>	<b>5</b>	<b>2</b>	<b>4</b>	<b>6</b>	<b>8</b>
H3 <sup>a</sup>	8.50	8.43	8.13	8.39	8.35	8.05	
H4	7.80	7.87	6.07	7.79	7.85	6.07	
H5	7.47	7.50	5.61	7.50	7.52	5.64	
H6	7.40	7.45	5.26	7.39	7.44	5.25	
H7	8.00	8.04	6.29	8.00	8.03	6.29	

H3 <sup>b</sup>	8.51	8.64	8.00	8.40	8.56	7.91	7.95
H4	7.33	7.50	5.03	7.31	7.48	5.00	5.11
H5	7.00	7.09	4.56	7.01	7.10	4.56	4.57
H6	6.95	7.02	4.19	6.94	7.00	4.17	4.15
H7	7.46	7.53	5.19	7.45	7.52	5.14	5.21

<sup>a</sup> spectrum was recorded in CDCl<sub>3</sub>

<sup>b</sup> spectrum was recorded in C<sub>6</sub>D<sub>6</sub>

A downfield shift in the resonances of the following pairs of complexes: **1? 3** or **2? 4** and **5? 7** or **6? 8** in C<sub>6</sub>D<sub>6</sub> is observed for the H3 chemical shift value in the <sup>1</sup>H NMR spectra of the complexes. The corresponding change in the structure of the complexes for these groupings is Et? TiCp<sub>2</sub>Cl, while the other substituents were kept the same. The observed downfield shift is ascribed to the electropositive Ti-fragment that withdraws electron density from the oxygen and forces the carbene carbon to “get” more electron density from the BT-substituent. This will influence the H3 proton in such a manner that H3 becomes more deshielded.

In grouping the following pairs of complexes: **1? 5** or **2? 6** and **3? 7** or **4? 8** and by studying their H3 chemical shift values in the <sup>1</sup>H NMR spectra in C<sub>6</sub>D<sub>6</sub> for these complexes, an upfield shift appears for every pair. The corresponding change in structure that appears in these pairs is BT? p-BTCr(CO)<sub>3</sub>, while the other substituent was kept the same. The observed upfield shift is ascribed to the Cr(CO)<sub>3</sub>-fragment which because of its coordination to BT retains electron density on the rings, causing the H3 proton to be more shielded. The same observations in the chemical shifts values in the <sup>1</sup>H NMR spectra of the complexes dissolved in CDCl<sub>3</sub>, were not observed.

In conclusion, the most dramatic downfield shift for H3 in the <sup>1</sup>H NMR spectra of the complexes is for **3** and **4**, demonstrating the electronic effect of the TiCp<sub>2</sub>Cl substituent and the most dramatic upfield shift for H3 is for **5** and **6**, demonstrating the electronic effect of the Cr(CO)<sub>3</sub> fragment.

The chemical shift of the carbonyl ligands in  $^{13}\text{C}$  NMR spectra are very insensitive to changes in the substituents of the carbene ligand and mostly effected only by the type of ligand and the number of carbonyl ligands attached to the metal.

**Table 6.2**  $^{13}\text{C}$  NMR Spectra<sup>a</sup> of complexes **1-5**

Carbon	Chemical shifts (d, ppm)				
	[Cr(CO) <sub>5</sub> ]-complexes			[W(CO) <sub>5</sub> ]-complexes	
	<b>1</b>	<b>3</b>	<b>5</b>	<b>2</b>	<b>4</b>
C1	320.5	324.5	318.2	294.3	-
C2	154.0	140.8	155.6	157.0	141.1
C3	141.9	139.5	138.2	142.5	139.4
C4	122.8	122.9	88.9	122.9	123.1
C5	128.9	128.4	89.8	128.8	128.4
C6	125.1	125.4	92.2	125.2	125.5
C7	126.8	126.9	84.3	126.9	127.1
C8, C9	138.7, 139.2	138.1	118.1, 126.6	139.0, 139.5	-
M(CO) <sub>5</sub>	216.9 (cis) 223.4 (trans)	217.9 (cis) 224.9 (trans)	216.5 (cis) 223.4 (trans)	197.5 (cis), (triplet) 202.6 (trans)	199.0 (cis)
M(CO) <sub>3</sub>	-	-	231.4	-	-

<sup>a</sup> spectrum was recorded in CDCl<sub>3</sub>

#### 4. Structural features of the carbene complexes

On comparing the structural data obtained for the complexes in the solid state, it is evident that the heteroaromatic ligand is planar and only very small distortions were observed for all of the complexes except **1** and **2**. With a planar heteroaromatic ligand, it is possible to facilitate the delocalization of electron density through the p-system of the ligand. In these Fischer carbene complexes, metal-metal communication through this delocalized system seems plausible. Bond lengths and angles surrounding the carbene carbon in solid state are

summarized in Tables 6.3 and 6.4. Figure 6.4 indicates the bond angles referred to in Table 6.4.

**Table 6.3** Selected bond lengths (Å) of the carbene complexes

Bond	[Cr(CO) <sub>5</sub> ]-complexes			[W(CO) <sub>5</sub> ]-complexes			
	<b>1</b>	<b>5</b>	<b>7</b>	<b>2</b>	<b>4</b>	<b>6</b>	<b>8</b>
M-C <sub>carb</sub>	2.067(3)	2.050(2)	2.077(4)	2.201(5)	2.211(4)	2.179(7)	2.207(4)
M-CO <sub>t</sub>	1.875(3)	1.884(3)	1.859(6)	2.018(6)	2.007(4)	2.011(7)	2.000(6)
M-CO <sub>av</sub>	1.9044(19)	1.905(3)	1.897(7)	2.036(4)	2.033(4)	2.058(8)	2.074(7)
C <sub>carb</sub> -O	1.319(3)	1.324(3)	1.285(5)	1.315(6)	1.279(4)	1.318(8)	1.280(5)
C <sub>carb</sub> -C	1.462(3)	1.472(3)	1.463(6)	1.468(7)	1.474(5)	1.471(8)	1.461(6)

carb = carbene, t = trans, av = average

The shortest metal-carbene distances, and these are significantly shorter, are associated with complexes **5** and **6** in solid state. This again highlights the role of the  $\pi$ -coordinated Cr(CO)<sub>3</sub> fragment within an arene carbene substituent and supports conclusions drawn from the NMR spectroscopy for these complexes in solution. The Cr(CO)<sub>3</sub> fragment retains the electronic charge on the BT-substituent and decreases the amount of charge transferred to the carbene carbon atom for **5** and **6** compared to the other complexes. As a result, more  $\pi$ -backdonation from the M(CO)<sub>5</sub> fragment is required to stabilize the electrophilic carbene carbon atom. One would expect the same observation for **7** and **8** because of the presence of the  $\pi$ -coordinated Cr(CO)<sub>3</sub> fragment, but instead these complexes represent the longest M-C(carbene) distances. This is ascribed to steric crowding around the carbene carbon atom that is greatest for **7** and **8** and would tend to lengthen the metal carbene distance to create more space for the bulky substituents. At the same time the M-CO(trans) bond increases its distance to compensate for the shorter M-C(carbene) distances. The metal-carbene distances fall within the range that are characteristic for alkoxy carbene complexes of M(CO)<sub>5</sub>.<sup>9</sup>

The shortest carbene-oxygen distances, and these are significantly shorter, are associated with complexes **4**, **7** and **8**. These complexes all display the very electropositive TiCp<sub>2</sub>Cl fragment on the one hand with a high affinity for the oxygen electron density, but this

fragment is the most bulky substituent surrounding the carbene carbon atom. As a result the C(carbene)-O and O-Ti distances are the net result of strong competition between TiCp<sub>2</sub>Cl fragment and the electrophilic carbene carbon for electron density on the one hand and steric interactions of the TiCp<sub>2</sub>Cl fragment on the other hand. This manifests in a short C(carbene)-O distance and a long Ti-O distance. The C(carbene)-C(BT) distances are the same for all the complexes, showing some delocalisation from the thienyl of the BT-substituent, but are more or less constant in magnitude.

A second aspect of importance is the bond angles surrounding the carbene carbon atom. These are shown in Figure 6.4 and the data given in Table 6.4. The sterically greatest substituent will impact on the two adjacent bond angles. From the data it is clear that the bond angle 2 remains more or less the same showing the very little steric interaction between the M(CO)<sub>5</sub> fragment and the BT-substituent. Especially important the fact that the introduction of the  $\pi$ -coordinated Cr(CO)<sub>3</sub> plays no role.

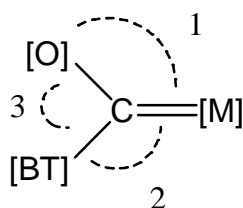


**Figure 6.4** Bond angles referred to in Table 6.4

**Table 6.4** Bond angles ( $^{\circ}$ ) shown in Figure 6.4 of the carbene complexes.

Angle	[Cr(CO) <sub>5</sub> ]-complexes			[W(CO) <sub>5</sub> ]-complexes			
	1	5	7	2	4	6	8
1	129.92(17)	130.04(15)	120.9(3)	130.1(4)	121.2(3)	130.0(4)	121.4(3)
2	124.89(17)	125.36(15)	126.4(3)	124.2(4)	125.9(2)	124.4(4)	121.4(3)
3	105.2(2)	104.52(18)	112.7(4)	105.7(4)	112.7(3)	105.5(5)	112.5(3)

The biggest steric effect is displayed in complexes **4**, **7** and **8** where the angles described by angle 1 are almost  $10^\circ$  smaller and those by angle 3 around  $8^\circ$  greater than the average values of the other complexes. In **4**, **7** and **8** the OEt-group was replaced by a much more bulky OTiCp<sub>2</sub>Cl-group and thus occupying a greater volume of space. Since the Cr(CO)<sub>3</sub>-fragment was relatively far away from the carbene carbon in comparison to the other metal centers, the occupied space at substituent 3 was not as crowded as that of substituent 2.

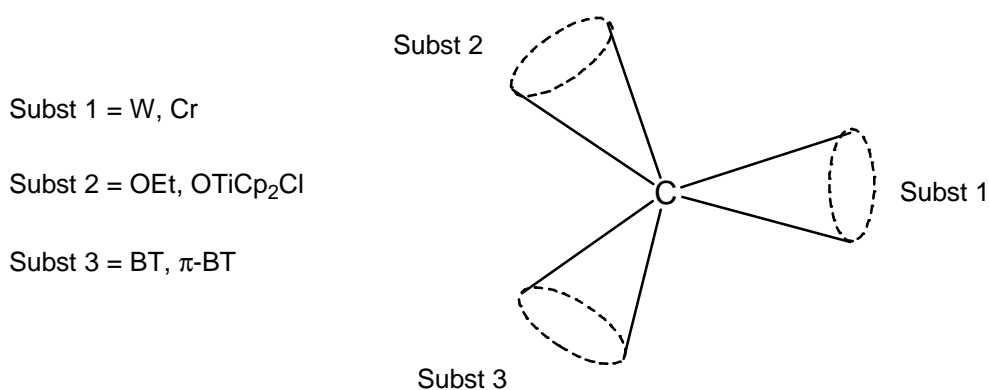


**Figure 6.5** Steric demands of metal substituents surrounding the carbene carbon

When looking closely at the structures of the synthesized complexes in the solid state, it appears as though there is some space available directly underneath the thiophene ring as indicated in Figure 6.6.

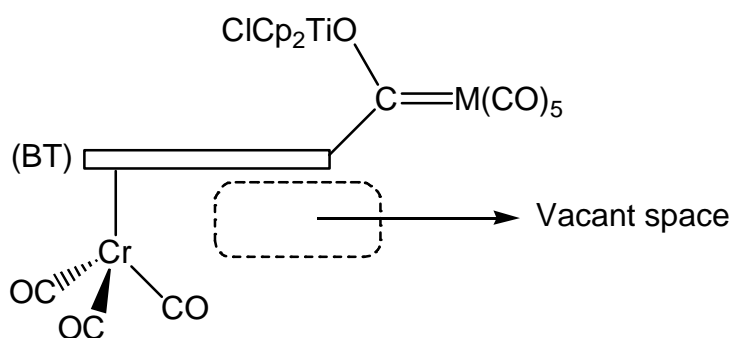


**Figure 6.6** Vacant space in synthesized trimetallic carbene complexes

In the quest to bind the metal-fragments as close as possible to the carbene carbon and evidently filling the "vacant space", one other complex was synthesized (**9**), containing a ferrocene fragment in the place of the p-BT, evidently forcing the iron metal centre to be closer to the carbene carbon than the chromium metal centre of the p-BT.

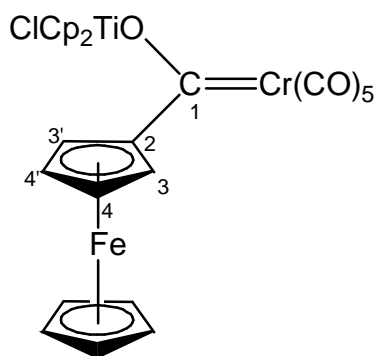


**Figure 6.7** Structural representation and numbering of carbene complex **9**

A fairly good spectrum was obtained for **9**, but as expected, this complex was less stable than the other previously synthesized trimetallic carbene complexes (**7** and **8**).

Chemical shifts (d, ppm,  $\text{CDCl}_3$ ) of **9**: 4.70 (H3 and H3'), 4.53 (H4 and H4'), 6.70 (Ti-Cp), 4.14 (Fe-Cp).

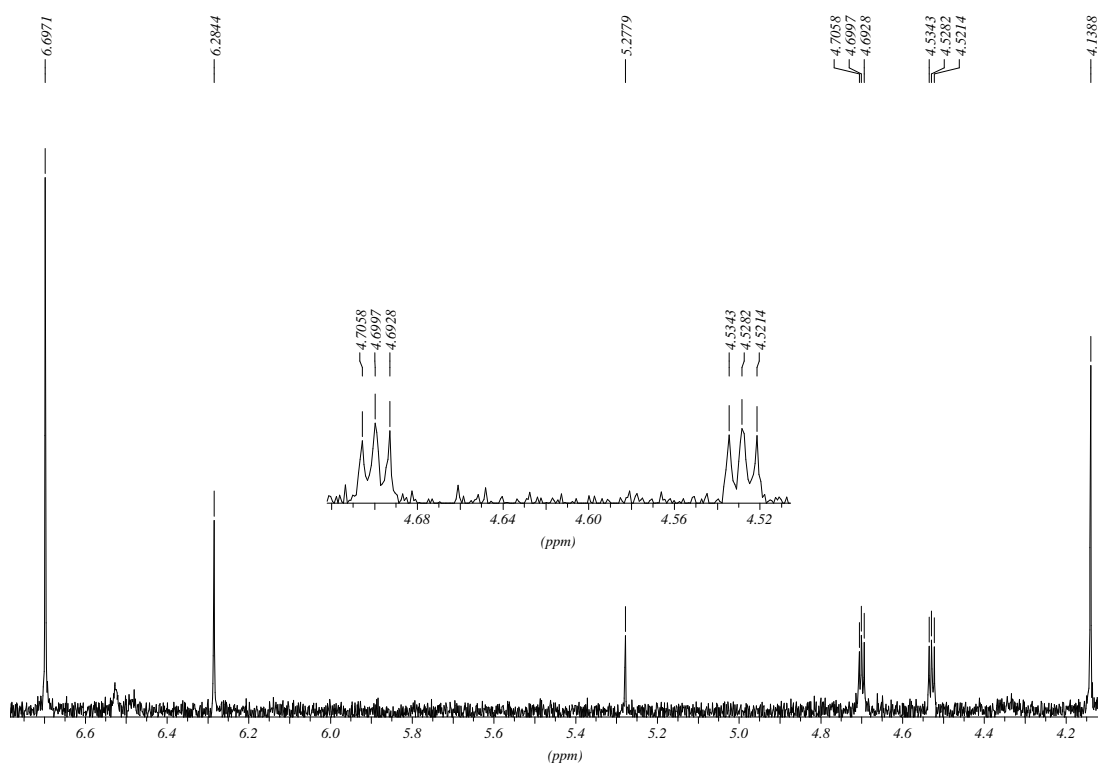


**Figure 6.8**  $^1\text{H}$  NMR spectrum of complex **9** in  $\text{CDCl}_3$

## 5. Future work

Many new opportunities exist to expand and study metal-containing carbene complexes. These refer to the following aspects:

- (i) Utilize open spaces (steric) and optimize electronic properties by introducing other metal  $\pi$ -coordinated fragments as substituents.
- (ii) Apply concept to Schrock carbene complexes, but to avoid steric complications using tetrahedrally coordinated metal substituents.
- (iii) Study reactivity patterns of the new trimetallic carbene complexes towards unsaturated C-C and C-X (X = heteroatom) bonds

## 6. References

1. U.Schubert, E.O.Fischer, *J. Organomet. Chem.* **1981**, 219 C34.
2. M.F.Semmelhack, R.Tamura, *J. Am. Chem. Soc.* **1983**, 105 4099.
3. R.B.Silverman, R.A.Olofson, *J. Chem. Soc. Chem. Commun.* **1968**, 1313.
4. E.O.Fischer, B.Heckl, K.H.Dötz, J.Müller, H.Werner, *J. Organomet. Chem.* **1969**, 16 29.
5. E.O.Fischer, D.Plabst, *Chem. Ber.* **1974**, 107 3326.
6. D.D.Graf, N.C.Day, K.R.Mann, *Inorg. Chem.* **1995**, 34 1562.
7. D.D.Graf, K.R.Mann, *Inorg. Chem.* **1997**, 36 141.
8. D.D.Graf, K.R.Mann, *Inorg. Chem.* **1997**, 36 150.
9. M.Sabat, M.F.Gross, M.G.Finn, *Organometallics* **1992**, 11 745.